

# Newly characterized motile sperm domain-containing protein 2 promotes human breast cancer metastasis

Yaniv Salem, Niva Yacov, Oshrat Propheta-Meirán, Eyal Breitbart and Itzhak Mendel 

VBL Therapeutics, Modi'in, Israel

Breast cancer is the most frequently diagnosed cancer and the leading cause of cancer death among women worldwide. Breast cancer metastasis results in poor prognosis and increased mortality, but the mechanisms of breast cancer metastasis are yet to be fully resolved. Identifying distinctive proteins that regulate metastasis might be targeted to improve therapy in breast cancer. We previously described MOSPD2 as a surface membrane protein that regulates monocyte migration *in vitro*. In this study, we demonstrate for the first time that MOSPD2 has a major role in breast cancer cell migration and metastasis. MOSPD2 expression was highly elevated in invasive and metastatic breast cancer while it was absent or residual in normal tissue and in primary *in situ* tumors. *In vitro* experiments showed that silencing MOSPD2 in different breast cancer cell lines significantly inhibited cancer cell chemotaxis migration. Mechanistically, we found that silencing MOSPD2 profoundly abated phosphorylation events that are involved in breast tumor cell chemotaxis. *In vivo*, MOSPD2-silenced breast cancer cells exhibited marked impaired metastasis to the lungs. These results indicate that MOSPD2 plays a key role in the migration and metastasis of breast cancer cells and may be used to prevent the spreading of breast cancer cells and to mediate their death.

## Introduction

Metastases are responsible for most cancer deaths.<sup>1</sup> The migration process of tumor cells from the primary site to local and remote sites consists of a series of steps, all of which must be successfully completed to give rise to a metastatic tumor. From the early stage of transforming from epithelial to mesenchymal, tumor cells become migratory and respond to extracellular cues that induce crossing the tumor cells' epithelial basement membrane, intravasation into the circulation and then extravasation into distant organs to form metastases.<sup>2,3</sup> In context of breast

**Key words:** MOSPD2, breast cancer, migration, metastasis

**Abbreviations:** CAS9: CRISPR-associated protein 9; CRISPR: clustered regularly interspaced short palindromic repeats; EGFR: epidermal growth factor receptor; ERK: extracellular signal-regulated kinases; MOSPD2: motile sperm domain-containing protein 2; sh-RNA: short hairpin RNA

Additional Supporting Information may be found in the online version of this article.

**Conflict of Interest:** The authors are employees and stock option holders of VBL Therapeutics.

**DOI:** 10.1002/ijc.31665

This is an open access article under the terms of the Creative Commons Attribution-NonCommercial-NoDerivs License, which permits use and distribution in any medium, provided the original work is properly cited, the use is non-commercial and no modifications or adaptations are made.

**History:** Received 8 Jan 2018; Accepted 12 Jun 2018; Online 6 Jul 2018

**Correspondence to:** Itzhak Mendel, Immunology Director, VBL Therapeutics, 8 Hasat St, Modi'in 7178106 Israel, Tel.: +972 8 9935000, Fax: +972 8 9935001, E-mail: itzhak@vblrx.com

cancer, a network of chemokines has been described that initiate and promote breast cancer cell migration. These chemokines include CXCL12, CCL21 and CX3CL1, all of which are expressed in the lung, liver, lymph nodes and bone, organs into which breast cancer cells disseminate preferentially.<sup>4-6</sup> At the same time, the counterpart receptors for these chemokines, CXCR4, CCR7 and CX3CL1, respectively, were shown to be overexpressed in metastatic breast tumor and cell lines and to promote breast cancer dissemination.<sup>4,6-8</sup> Induction of breast cancer cell metastasis is not contingent to chemokines only and can also be attributed to growth factors, in particular epidermal growth factor (EGF), which interacts with receptor tyrosine kinase (RTK) epidermal growth factor receptor (EGFR). Engagement of chemokine receptor or RTK induces phosphorylation and downstream signaling events, including the PI3K-AKT and MEK-ERK pathways, which are fundamental for chemotaxis directed migration.<sup>9-11</sup> Given the influence of chemokines on a range of processes associated with cancer metastases, it was expected that the use of chemokine antagonists would have a beneficial effect. Whereas pre-clinical studies targeting chemokine receptors or their ligands significantly inhibited breast cancer metastasis,<sup>12,13</sup> none of these treatments are implemented in clinical settings.

Motile sperm domain-containing protein 2 (MOSPD2) is a single-pass membrane protein to which no function was ascribed up until recently. We showed previously that MOSPD2 is expressed on the plasma membrane of human monocytes and that targeting of MOSPD2 inhibits their migration without affecting proliferation.<sup>14</sup> We therefore hypothesized that MOSPD2 also promotes metastasis of cancer cells. Human Protein Atlas and TCGA data bases show

**What's new?**

Motile sperm domain-containing protein 2 (MOSPD2) is a key regulator of monocyte migration and is suspected of promoting cancer cell metastasis. In cancer patients, its expression is inversely correlated with survival. Here, MOSPD2 expression was found to be significantly elevated in metastatic breast cancer cells, with no or only residual expression in normal tissues and primary *in situ* tumors. *in vitro* MOSPD2 silencing inhibited breast cancer cell migration and impeded migration-associated phosphorylation events. Its silencing *in vivo* impaired metastasis to the lungs, suggesting that MOSPD2 inhibition could be a useful therapeutic strategy for metastatic breast cancer in human patients.

that MOSPD2 RNA is detected in all cancer types and its expression is in inverse correlation to survival (<https://www.proteinatlas.org/ENSG00000130150-MOSPD2/pathology>). The abundance of MOSPD2 was initially evaluated using a tumor microarray covering a wide range of cancer types. MOSPD2 was detected in the majority of cancerous organs, at concentrations that were higher than those found in normal tissue. Since breast cancer is one of the more experimentally studied cancers, tumor microarrays containing samples from different stages of the disease were tested, revealing that MOSPD2 prevalence is correlated with disease progression. Silencing gene expression in different breast cancer cell lines significantly inhibited migration and invasion as well as downstream EGFR signaling cascades *in vitro* without affecting cell proliferation. *In vivo*, MDA-231 cells with silenced MOSPD2 displayed impaired ability to disseminate to the lungs. Taken together, we suggest that MOSPD2 regulates migration and metastasis of breast cancer cells and is a potential target for the treatment of metastatic breast cancer.

**Materials and Methods****Mice**

Female 8- to 10-week-old SCID (C.B-17/IcrHsd-Prkdcscid) mice were purchased from Harlan Laboratories, Israel. All experiments were approved by the Institutional Animal Care and Use Committee of the Sheba Medical Center, Ramat Gan, Israel.

**MOSPD2 silencing**

Human breast cancer cell lines MDA-MB-231 (hereafter MDA-231) (ATCC<sup>®</sup> HTB-26<sup>TM</sup>), BT-20 (ATCC<sup>®</sup> HTB19<sup>TM</sup>) and ZR-75-1 (ATCC<sup>®</sup> CRL-1500<sup>TM</sup>) were purchased from ATCC. The cells were used in the described experiments between 2 and 6 weeks from thawing. Cells ( $2 \times 10^6$  in 2 mL) were placed in a 15 mL tube and lentiviral particle-expressing control short hairpin RNA (sh-Control) (SHC202V, Sigma, Israel) or human MOSPD2 (sh-MOSPD2) Exon 4 (TRCN0000323142 Sigma) were applied on the cells, which were then spun for 60 min at 2,000 rpm at room temperature in the presence of 8 µg/mL polybrene (Sigma). The cells were then seeded in a 6-well plate. After 72 hr, fresh medium containing puromycin (4 µg/mL Sigma) was added for the selection of transduced cells. For CRISPR-CAS9 (hereafter CRISPR)-mediated silencing, cells were transduced with CRISPR non-target control (CRISPR-Control) (CRISPR12V, Sigma), CRISPR human MOSPD2 Exon 3 (CRISPR-MOSPD2) (HS0000528665, Sigma) or Exon

9 (HS0000176080, Sigma) lentiviral particles as described above. Single-cell cloning was performed on CRISPR-transduced cells to isolate cells with silenced MOSPD2 protein expression.

**Generation of anti-MOSPD2 polyclonal antibody**

Rabbits were immunized with approximately 0.5 mg of HA-rh MOSPD2 emulsified in complete Freund's adjuvant followed by three boosts every 3 weeks of approximately 0.25 mg of HA-rh MOSPD2 emulsified in incomplete Freund's adjuvant. Serum was collected 1 week after each boost for immunogenicity assessment and titers. α-MOSPD2 antibodies were isolated from serum using protein A/G beads (Santa Cruz Biotechnology, CA).

***In vitro* trans-well migration and invasion assay**

To test for trans-well migration, sh-Control or sh-MOSPD2 transduced cells ( $3 \times 10^5$ ), previously starved for 3 hr in 0.5% FBS/RPMI-1640, were seeded in the upper chamber of a QCM 24-well, 5 µm pores, migration assay plate (Corning-Costar, Corning, NY), followed by incubation for 24 hr in the presence of 10% FBS/RPMI-1640 and EGF (20–200 ng/mL, Peprotech, Israel) in the lower chamber. Cells that migrated to the lower compartment were subsequently stained with crystal violet before images were taken. Cells transduced with CRISPR-Control or MOSPD2 lentiviral particles were similarly treated and tested for migration. In addition, Control-transduced or MOSPD2 CRISPR-transduced MDA-231 cells ( $3 \times 10^5$ ) were counted in the lower chamber using FACS. The 96-well CULTREX<sup>®</sup> 3D Culture BME Cell Invasion Assay was used for the 3D spheroid invasion assay according to manufacturer's protocol. Cells were harvested, counted and mixed with 10× Spheroid Formation ECM and medium. Then, 50 µL of the single cell suspension in 1× Spheroid Formation ECM were added to each well of the 3D Culture Qualified 96 Well Spheroid Formation Plate in triplicates. The plate was centrifuged at 200g for 3 min at room temperature in a swinging bucket rotor and incubated at 37°C for 72 hr to promote spheroid formation. After 72 hr, the 96-well 3D Culture Qualified Spheroid Formation Plate was incubated on ice for 15 min to cool the wells. Working on ice, 50 µL of Invasion Matrix was added to each well in the Formation Plate. The plate was centrifuged at 300g at 4°C for 5 min in a swinging bucket rotor to eliminate bubbles and position spheroids in the Invasion Matrix toward the middle of the well. After 1 hr, 100 µL of warm cell culture medium (37°C) with 20% FBS and 20 ng EGF was added and left to rest for 3–6 days at 37°C.

The spheroid in each well was photographed every 24 hr using a 4× objective.

### Cell proliferation

For cell proliferation in culture medium, cells transduced with sh-Control or sh-MOSPD2 lentiviral particles were seeded in 6-well plates ( $10^4$  per well). The cells were counted in triplicate by FACS every 24 hr for three consecutive days. To measure proliferation within the spheroid, cells were seeded as described above in the 96-well CULTREX<sup>®</sup> 3D Culture BME proliferation assay. After 3 days, 50  $\mu$ L of warm cell culture medium (37°C) was added to enable proliferation. To measure mitochondrial activity as an indicator of live cells, 10  $\mu$ L of Resazurin was added for an additional 24 hr at 37°C, after which 100  $\mu$ L of detergent reagent was added for an additional 24 hr. Absorbance was read at 570 nm.

### Western blotting

Cells ( $10^6$ ) were washed and re-suspended in lysis buffer containing 1:100 dithiothreitol (DTT), and phosphatase and protease inhibitors (Thermo Scientific, MA). Samples were loaded onto a precast Criterion TGX gel (Bio-Rad, Hemel Hempstead, UK) and transferred onto nitrocellulose membrane. Blots were blocked with 5% milk or BSA in Tris-buffered saline and Tween 20 (TBST) for 1 hr, followed by incubation with primary and secondary antibodies. Membranes were developed using an ECL kit (Thermo Scientific). The following antibodies were used for immunoblotting.

**Primary antibodies.** Rabbit anti-MOSPD (1:5,000) was generated in-house. Phospho-extracellular-regulated kinase (p-ERK1/2) (Thr 183 and Tyr 185, 1:4,000) and phospho-EGFR (Y-869 1:1000) were purchased from Sigma (Israel). Phospho-AKT (Ser 473, 1:1,000), phospho-EGFR (Y1068 and Y1173, 1:1,000), EGFR (1:1,000), phospho-GAB1 (Y659 1:1,000), phospho-SHP-2 (1:1,000) and phospho-p38 (1:1,000) were purchased from Cell Signaling, MA. Phospho-EGFR (Y845 1:1,000) was purchased from EMD Millipore, MA. Heat shock protein (HSP) 90 (1:1,000) was purchased from Santa Cruz Biotechnology (TX).

**Secondary antibodies.** HRP donkey anti-rabbit (1:5,000) and HRP goat anti-mouse (1:5,000) were purchased from Jackson ImmunoResearch (West Grove, PA).

### Tissue microarray staining and image analysis

To assess the prevalence of MOSPD2, tissue arrays of multiple organ tumor tissue and normal tissue MC6163, and normal tissue and breast cancer T088B and BR2082a tumor microarrays (US Biomax Rockville, MD) were stained with validated rabbit anti-MOSPD2 Prestige antibody<sup>®</sup> (1:80, Sigma) or control rabbit antibody (R&D Systems) for 40 min, after which an ultra-View Universal DAB Detection Kit (Ventana Medical Systems, 760-500) was applied. MOSPD2 abundance was scored

according to Junttila *et al.*<sup>15</sup> who defined semi-quantitative IHC scores on a scale of 0–3, where 0 means no staining, 1 is weak, 2 is moderate and 3 is strong staining. When heterogeneous staining within a single core was observed, the score referred to the area with the highest coverage. Scoring was performed by two individual scientists in a blinded fashion.

### *In vivo* breast cancer models and metastasis assessment

**Systemic.** MDA-231 ( $10^6$ ) CRISPR-Control or CRISPR-MOSPD2 isolated clone 14 cells were injected into the tail veins of 8-week-old female SCID mice (C.B-17/IcrHsd-Prkdc<sup>scid</sup>, Harlan). Mice were sacrificed after 4 weeks. Lungs were excised for histopathologic examination.

**Orthotopic.** MDA-231 cells ( $5 \times 10^6$ ) transduced with sh-Control or sh-MOSPD2 lentiviral particles were injected into the mammary fat pads of 8-week old female SCID mice (C.B-17/IcrHsd-Prkdc<sup>scid</sup>, Harlan). Mice were sacrificed after 10 weeks. Ipsilateral inguinal lymph nodes and lungs were excised for examination.

Histology slides were stained with hematoxylin/eosin (H&E). Formalin-fixed lungs were dehydrated, embedded in paraffin, and sectioned at 4  $\mu$ m thickness. The H&E staining was calibrated on a Leica staining module. The slides were warmed to 90°C for 7 min and then processed according to a fully automated protocol. After sections were dewaxed and rehydrated, slides were stained for 7 min in Gill's Hematoxylin No. 3 (Surgipath), washed, dipped in acidic alcohol and washed. After short dipping in 70% ethanol and 96% ethanol, slides were stained for 4 min in Eosin (Sigma), and dehydrated in 96% ethanol and then twice in 100% ethanol for 1 min each time. After automated staining run was completed, sections were cleared in xylene for 10 s and mounted with Entellan.

### Statistical analysis

Data were analyzed using SigmaPlot 12. Student's *t* test or Mann–Whitney test were used for comparisons between the two groups.

### Results

#### MOSPD2 is highly expressed in malignant and metastatic breast cancer

The prevalence of MOSPD2 was initially assessed in multiple organ tumors and normal tissue. MOSPD2 expression was evident in the majority of organ tumors (15/19) including colon, esophagus, liver and breast (Fig. 1a and Table 1). Furthermore, with the exception of testis, normal tissue was either devoid of MOSPD2 or had a lower mean score than its parallel tumor tissue (Table 1). Breast cancer is one of the more experimentally studied tumors, with ample data generated from various cell lines and animal models. To reinforce breast cancer staining data obtained from the multiorgan array, the prevalence of MOSPD2 was assessed using tissue microarrays containing breast-only cores of one normal tissue,

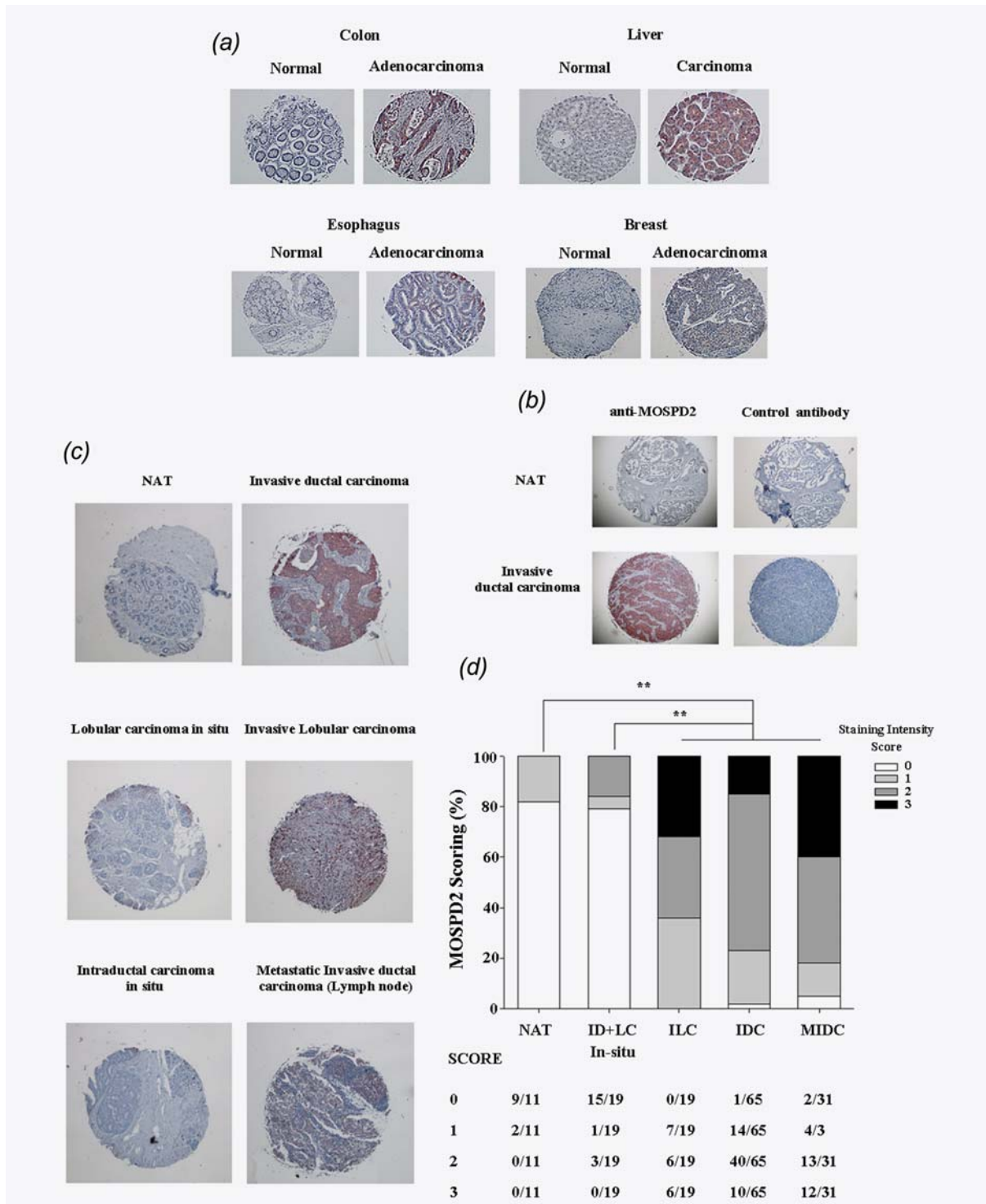


Figure 1. MOSPD2 is highly prevalent in invasive breast cancer tissue. (a) Tissue arrays of multiple organ tumor and normal tissues were stained with antibody to human MOSPD2, as described in “Materials and Methods.” Representative staining of various normal and tumor organs is presented. One of two independent stained arrays is shown. (b) Breast cancer tissue array containing normal, NAT and invasive ductal carcinoma tissue was stained with anti-MOSPD2 antibody or control antibody. Representative staining is shown. (c) Examples from breast cancer tissue array representing the abundance of MOSPD2 in NAT, primary, invasive and metastatic breast cancer tissue stained with anti-MOSPD2 antibody. (d) Scoring summary based on staining intensity of MOSPD2 from pathology diagnosis groups shown in c. NAT, normal adjacent tissue; ID, intra-ductal carcinoma; LC, lobular carcinoma; ILC, invasive lobular carcinoma; IDC, invasive ductal carcinoma; MIDC, metastatic invasive ductal carcinoma.  $**p \leq 0.001$ . [Color figure can be viewed at [wileyonlinelibrary.com](http://wileyonlinelibrary.com)]

**Table 1.** Results of IHC MOSPD2 staining of multiple organ tumor and normal tissue microarray

Organ	Number of MOSPD2 <sup>+</sup> samples (%) and mean intensity score	
	Normal/NAT	Cancer
Bladder	0/7 (0)	0/20 (0)
	0	0
Cerebrum	0/8 (0)	0/20 (0)
	0	0
Breast	0/7 (0)	5/20 (25)
	0	0.25
Colon	0/7 (0)	7/9 (78)
	0	1.40
Esophagus	0/8 (0)	10/20 (50)
	0	0.65
Head and neck	0/8 (0)	3/20 (15)
	0	0.15
Kidney	0/8 (0)	6/19 (31.6)
	0	0.37
Liver	0/8 (0)	9/20 (45)
	0	0.60
Lung	0/8 (0)	7/48 (14.5)
	0	0.17
Lymph node	0/8 (0)	0/20 (0)
	0	0
Ovary	0/8 (0)	6/20 (30)
	0	0.41
Pancreas	1/8 (12.5)	7/20 (35)
	0.13	0.40
Prostate	0/6 (0)	0/22 (0)
	0	0
Soft tissue	0/8 (0)	5/9 (56)
	0	0.67
Stomach	0/8 (0)	0/20 (0)
	0	0
Testis	5/7 (71)	1/20 (5)
	0.71	0.10
Thyroid gland	2/8 (25)	10/20 (50)
	0.25	0.57
Uterine cervix	0/8 (0)	5/20 (25)
	0	0.20
Uterus	4/8 (50)	14/18 (78)
	0.50	1.06

one normal adjacent tissue (NAT), and invasive ductal carcinoma grade 2 taken from four different subjects. Strong MOSPD2 staining was detected in all four samples of invasive ductal carcinoma when compared to staining with control antibody, whereas none of the two normal tissue and NAT samples tested positive (Fig. 1b). Next, we searched for a correlation

between the level of MOSPD2 expression and the pathology diagnosis/stage, ER, PR or HER markers using tumor microarray that included an extended number of cases. While we could not establish a correlation between MOSPD2 staining intensity and the expression of ER, PR or HER, we found a clear correlation between staining intensity and the degree of invasiveness (Fig. 1c). No staining was obtained in 82% of the NAT samples, while the remaining 18% percent displayed a staining intensity of 1. In the cores pathologically characterized as carcinoma in situ, 79% of samples displayed no staining, while the remaining 21% scored 1 or 2. However, compared to NAT and carcinoma in situ tissue, invasive and metastatic tissues demonstrated a higher frequency of staining intensity 2 as well as staining intensity scores of up to 3 (Fig. 1d). Thus, the combined scores of staining intensities 2 and 3 for invasive lobular carcinoma, invasive ductal carcinoma and metastatic invasive ductal carcinoma were 63% (12/19), 77% (50/65) and 81% (25/31), respectively. These results indicate that MOSPD2 prevalence may be associated with the transition of breast cancer cells from being locally restricted to being invasive.

#### MOSPD2 is required for the migration and invasion of breast cancer cells *in vitro*

We previously silenced the expression of MOSPD2 in human monocytes using sh-RNA lentiviral particles targeting two different exons, 4 and 14, with the former being more efficient.<sup>14</sup> To investigate whether MOSPD2 is required for the migration and invasion of breast tumor cells, its expression was first silenced in the basal MDA-231 breast cancer cell line using sh-MOSPD2 lentiviral particles targeting exon 4 (Fig. 2a). The cells were then tested in a trans-well migration assay in the presence of EGF, which was previously reported to strongly promote chemotaxis but not proliferation of MDA-231 breast cancer cells.<sup>16,17</sup> The results depicted in Figure 2a show that MOSPD2-silenced MDA-231 breast cancer cells were severely impaired in their ability to migrate toward a medium containing EGF *in vitro*. This effect was not due to attenuated proliferation, as MOSPD2-silenced cells proliferated at a comparable rate to control cells (Fig. 2b). Periodic evaluation of the silenced cells revealed, however, that with time, MOSPD2 escape variants emerge. In an attempt to institute durable silencing, we transduced MDA-231 cells with CRISPR-lentiviral particles that target exon 3 or exon 9 of the MOSPD2 gene. Following cloning, isolated clones were examined for *in vitro* migration using EGF for chemoattraction. Figures 2c–2e present data for three clones, Nos. 7, 14 and 17, which were isolated from exon 3 targeted MOSPD2-silenced cells, compared to control transduced cells. Sequencing of these clones showed that the CRISPR-MOSPD2 DNA target region for Clone 7 was not altered, while Clones 14 and 17 harbored nucleotide deletions and mismatches (Supporting Information Fig. S1). When MOSPD2 protein was assessed, Clone 7 demonstrated higher MOSPD2 levels than CRISPR-Control transduced cells, whereas Clones 14 and 17 displayed

extremely low MOSPD2 levels, with Clone 14 exhibiting the lowest level (Fig. 2c). Clone 7 migrated in higher numbers than did control transduced cells, whereas Clones 14 and 17 demonstrated a profoundly impaired ability to migrate (Figs. 2d and 2e). Reduced migration was also observed when MOSPD2 expression was silenced in MDA-231 cells by targeting exon 9 (Figs. 2f and 2g). All CRISPR-MOSPD2 silenced cells subsequently used were targeted in exon 3. Taken together, these results indicate that the extent of migration of MDA-231 breast cancer cells *in vitro* is in direct correlation with the expression level of MOSPD2, which is not involved in cell proliferation. Next, we assessed whether MOSPD2 is essential for migration of breast cancer cell lines other than MDA-231 and for invasion. To that end, a basal BT-20 breast cancer cell line was MOSPD2 silenced by sh-lentiviral particles and tested for migration. Figure 2h shows that silencing MOSPD2 in BT-20 profoundly inhibited their migration toward EGF. Tumor cell dissemination involves intra- and extravasation through the extracellular matrix. We therefore also tested the effect of MOSPD2 deficiency on chemotaxis migration of breast cancer cells in invasion matrix. In MDA-231 cells, silencing of MOSPD2 profoundly abrogated their ability to traverse the invasion matrix without affecting their proliferation (Figs. 3a and 3b). ZR-75-1 is a luminal (ER<sup>+</sup>) breast cancer line of cells that is capable of traversing invasion matrix. Figure 3c shows that invasion of MOSPD2-silenced ZR-75-1 cells was completely suppressed.

#### MOSPD2 promotes EGF-induced signaling events in breast cancer cells

Ligation to EGFR induces a cascade of signaling events that involve phosphorylation downstream of the receptor and results in protrusions required for directional migration. We sought to investigate the molecular basis for MOSPD2's role in breast cancer cell migration by assessing initiation and/or ensuing signals driven by EGFR. When CRISPR-Control MDA-231 cells were activated with EGF, all tested proteins, from the receptor itself (Y1068) to those directly recruited to the EGFR, GAB1 and SHP-2, as well as downstream p38 and AKT, were phosphorylated. The extent of ERK phosphorylation was examined, but due to high baseline phosphorylation levels, no activation could, by and large, be observed. Yet, upon activation of CRISPR-MOSPD2 silenced cells with EGF, phosphorylation of all tested proteins excluding p38 was markedly inhibited (Fig. 4a). To determine whether impaired signaling events subsequent to EGF ligation were common to different breast cancer cell lines in which MOSPD2 expression is abrogated, control or MOSPD2-silenced BT-20 or ZR-75-1 cell lines were activated with EGF and examined for downstream cues. Figures 4b and 4c demonstrate that phosphorylation of EGFR, as well as of AKT and ERK, was reduced in MOSPD2-silenced cells. IGF is another growth factor that is also associated with breast cancer invasion. In contrast to EGF-induced activation, ligation of IGF-1 induced

comparable AKT phosphorylation in CRISPR-Control and CRISPR-MOSPD2 MDA-231 cells (Fig. 4d), suggesting a degree of specificity in which receptor tyrosine kinase is functionally associated with MOSPD2. Ligation of EGF induces phosphorylation of the receptor on tyrosine residues other than Y1068. An analysis of some of those sites revealed that phosphorylation was profoundly decreased on all tested tyrosine residues of EGFR in MOSPD2-silenced cells. Attenuated phosphorylation was not due to reduced expression of EGFR (Fig. 4e).

#### MOSPD2 promotes breast cancer cell metastasis

Next, we studied the role of MOSPD2 in breast cancer cell metastasis. To that end, SCID mice were injected orthotopically with sh-Control or sh-MOSPD2 MDA-231 cells. On the day of sacrifice, ipsilateral lymph nodes from mice injected with sh-MOSPD2 MDA-231 cells were profoundly smaller than those excised from mice injected with sh-Control transduced cells (Fig. 5a). These results indicate that a smaller number of tumor cells traveled from the injection site to the draining lymph node. Moreover, the area covered by metastases in the lungs was significantly smaller in mice injected with sh-MOSPD2 (Fig. 5b) but the size of the primary tumor was not significantly different between the groups (Fig. 5c). We also examined the effect of MOSPD2 silencing on lung metastases following injection of MDA-231 CRISPR-Control or CRISPR-MOSPD2 isolated clone 14 cells. The results demonstrate that the tumor burden in the lungs of mice transferred with CRISPR-MOSPD2 clone 14 cells was significantly lower compared to control mice (Figs. 5d and 5e).

#### Discussion

The spread of cancer cells outside the inception site involves receptor activation that promotes dissemination of cells to other tissues. Preventing cancer cells from metastasizing remains an extremely challenging task, and identifying new therapeutic targets that inhibit migration and metastasis of tumor cells could prove beneficial. MOSPD2, which was recently found to play an essential role in human monocyte migration, was explored for its potential to regulate cancer cell migration and metastasis. We initially found that MOSPD2 is induced in many types of cancer, whereas it is absent or significantly less abundant in normal tissue. When further investigated in breast cancer tissues, MOSPD2 levels were correlated with the stage of invasiveness, that is, absent or residual in normal breast tissue, mildly increased at the early stage of *in situ* carcinoma and profoundly elevated in invasive and metastatic breast cancer. Intense MOSPD2 staining in breast cancer tissue appeared to be located primarily in the intracellular compartment. Whether this is a display of the full-length MOSPD2 or a different isoform of the protein is still under investigation. Nonetheless, MOSPD2 expression was not restricted to the intracellular compartment as cell fractionation and staining by flow cytometry showed that

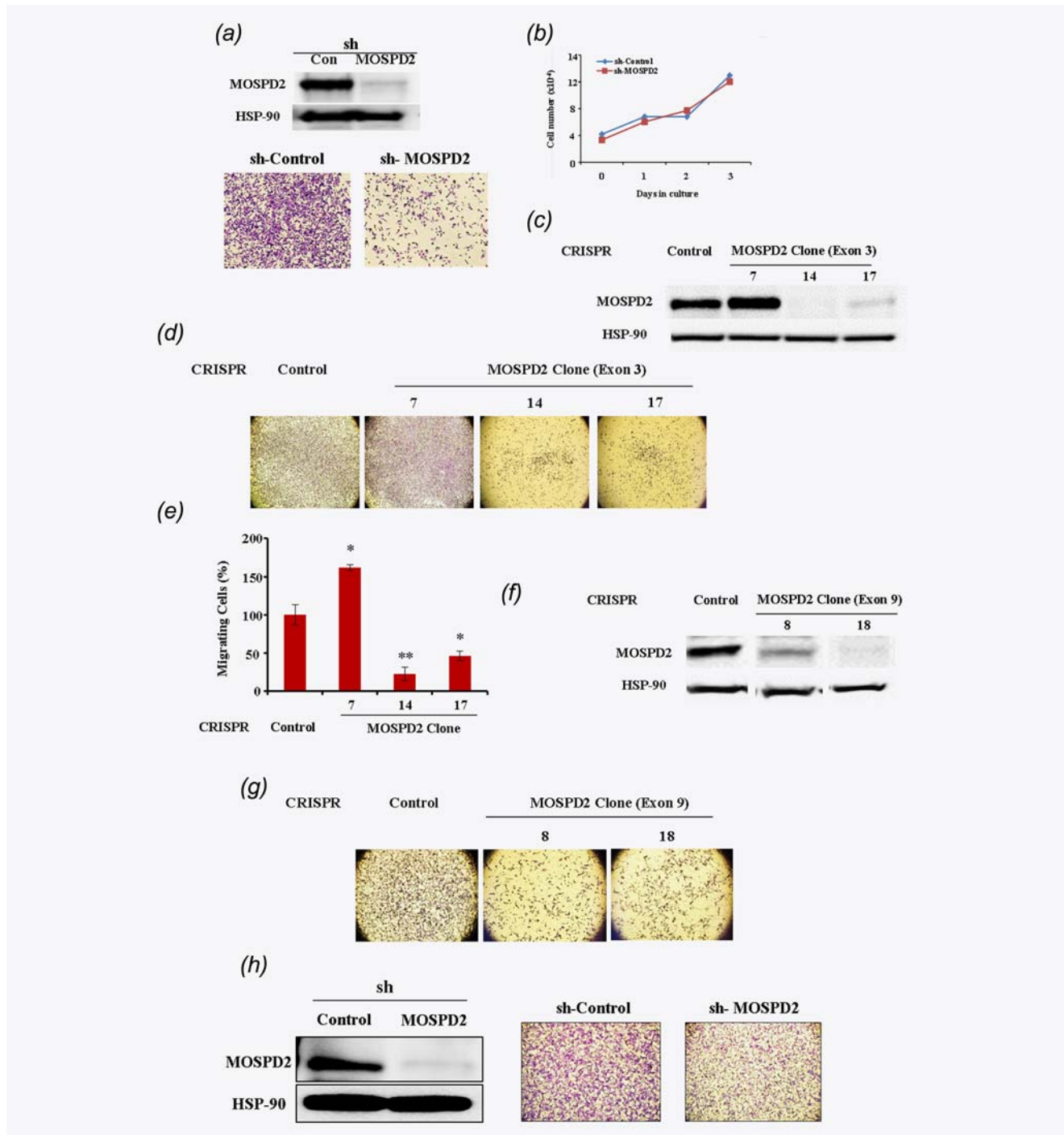


**Figure 2.** Mospd2 promotes migration of breast cancer cells. (a) Western blot for the detection of MOSPD2 protein using anti-MOSPD2 antibody on MDA-231 breast cancer cells transduced with sh-Control or sh-MOSPD2 lentiviral particles and trans-well migration toward EGF (200 ng/mL) of these cells, as described in “Materials and Methods.” Photos of well bottoms are shown. One of four experiments is presented. (b) Proliferation assay of sh-Control vs. sh-MOSPD2-treated MDA-231 cells. One of two experiments is shown. (c) Western blot for the detection of MOSPD2 protein expression on clones derived from MDA-231 cells transduced with CRISPR-Control or CRISPR-MOSPD2 lentiviral particles targeting exon 3. (d) Trans-well migration of clones in c. Photos of well bottoms are shown. One of three experiments is presented. (e) Enumeration of cells in d by flow cytometry. (f) Western blot for the detection of MOSPD2 on clones derived from MDA-231 cells transduced with CRISPR-Control or CRISPR-MOSPD2 lentiviral particles targeting exon 9. (g) Trans-well migration of clones in f. Photos of well bottoms are shown. One of three experiments is presented. (h) Western blots and trans-well migration of sh-Control compared to sh-MOSPD2-silenced BT-20 cells. Photos of the lower part of the membrane are shown. One of three experiments is presented. \* $p < 0.05$ , \*\* $p \leq 0.001$ . [Color figure can be viewed at [wileyonlinelibrary.com](http://wileyonlinelibrary.com)]

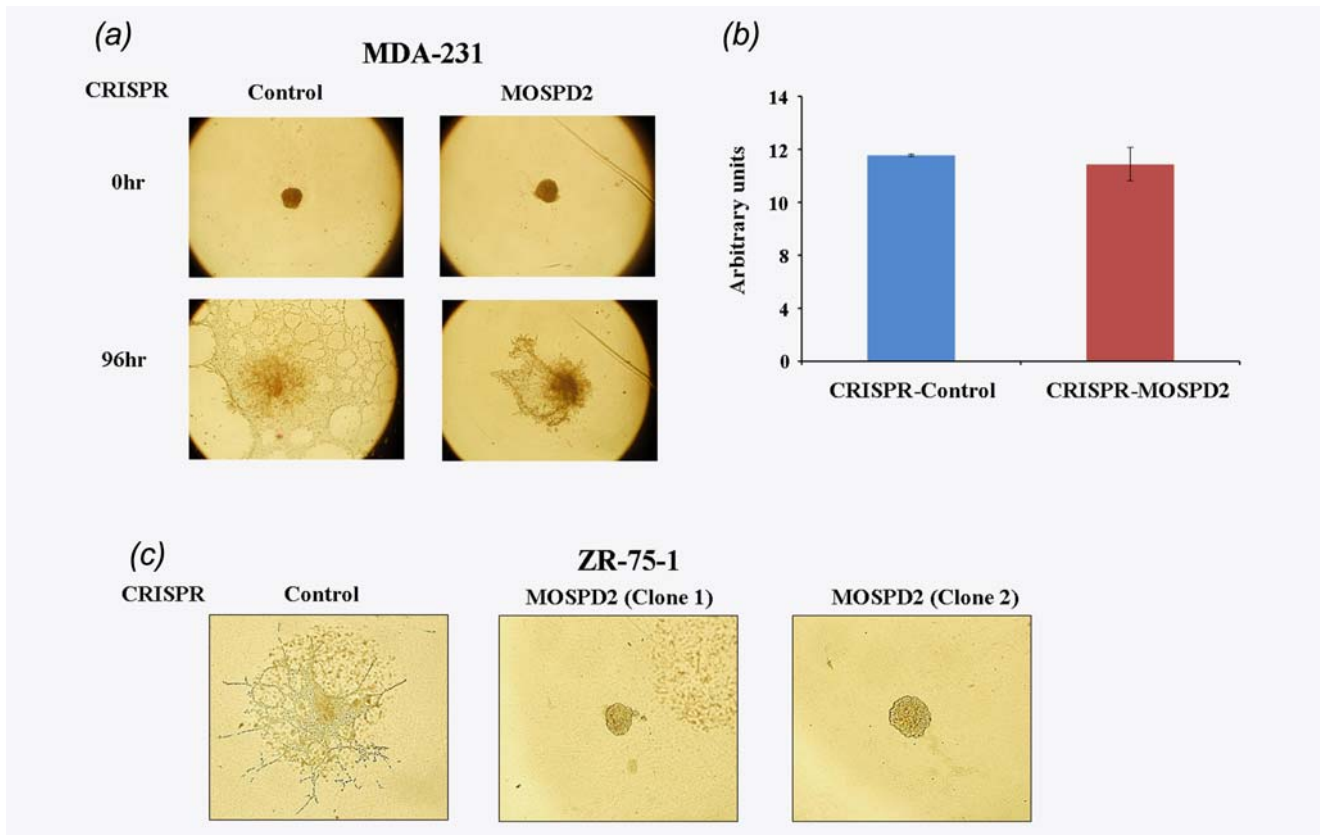


**Figure 3.** MOSPD2 is essential for invasion of breast cancer cells. MDA-231 (a) or ZR-75-1 (c) cell lines were transduced with CRISPR-Control or CRISPR-MOSPD2 lentiviral particles. Control and MOSPD2-silenced clones were tested using a 3D spheroid invasion assay for their ability to transverse the basement membrane matrix in medium containing 20% FBS and EGF 20 ng/ml for 3 days for MDA-231 or 6 days for ZR-75-1 cells. (b) Proliferation assay of CRISPR-Control vs. CRISPR-MOSPD2-treated MDA-231 cells in the spheroid. One of two experiments is shown. The results shown are expressed as mean  $\pm$  SD. [Color figure can be viewed at [wileyonlinelibrary.com](http://wileyonlinelibrary.com)]

MOSPD2 is also present on the plasma membrane (Supporting information Fig. S2), suggesting potential relevance for MOSPD2 as a therapeutic target for treatment with antibodies or small molecules. Even though MOSPD2 did not promote MDA-231 cell line proliferation *in vitro* and the primary tumor volume *in vivo* was largely comparable between control and MOSPD2-silenced groups, the reduced size of lymph nodes and the lower number of lung metastases excised from mice inoculated with MOSPD2-silenced cells further support the important role MOSPD2 plays in promoting metastasis.

The striking effect that MOSPD2 silencing had on the migration of breast cancer cells warranted further exploration of the molecular basis of its function. We found that the initial event subsequent to ligation of EGF, that is, autophosphorylation of EGFR at tyrosine 1068, is impaired in MDA-231 cells. Indeed, all downstream signaling pathways were expected to be perturbed. This was true for the most part, as phosphorylation of proteins that are recruited to the EGFR or the downstream AKT, a paramount mediator of migration, was markedly affected in MDA-231 cells. However, phosphorylation of p-38

was not altered by MOSPD2 silencing, thus indicating a degree of selectivity in its regulation of EGFR activation. Nonetheless, testing the effect of MOSPD2 silencing on other tyrosine residues of the EGFR following EGF binding showed decreased phosphorylation as well. Further support for the functional specificity of MOSPD2 came from the effect on signaling induced by IGF-1. Activation of the IGF-1 receptor (IGF-1R), which also belongs to the RTK family, triggers phosphorylation of AKT<sup>18</sup> and IGF-1R is implicated in the adhesion, invasion, and metastasis of breast cancer cells.<sup>19</sup> However, in contrast to the effect observed with EGF-induced signaling, IGF-1R-driven phosphorylation of AKT was not altered in MOSPD2-silenced MDA-231 cells. This result indicates that MOSPD2 does not promote activation of RTK indiscriminately. Perturbed migration and impaired phosphorylation of the EGFR and sequential signaling events was not unique to MDA-231 cells and was observed also in two other MOSPD2-silenced breast cancer cell lines, the basal BT-20 and luminal ZR-75-1. We, therefore, suggest that MOSPD2 is generally implicated in breast carcinogenesis and is a potential target for the treatment of breast cancer of different classifications.

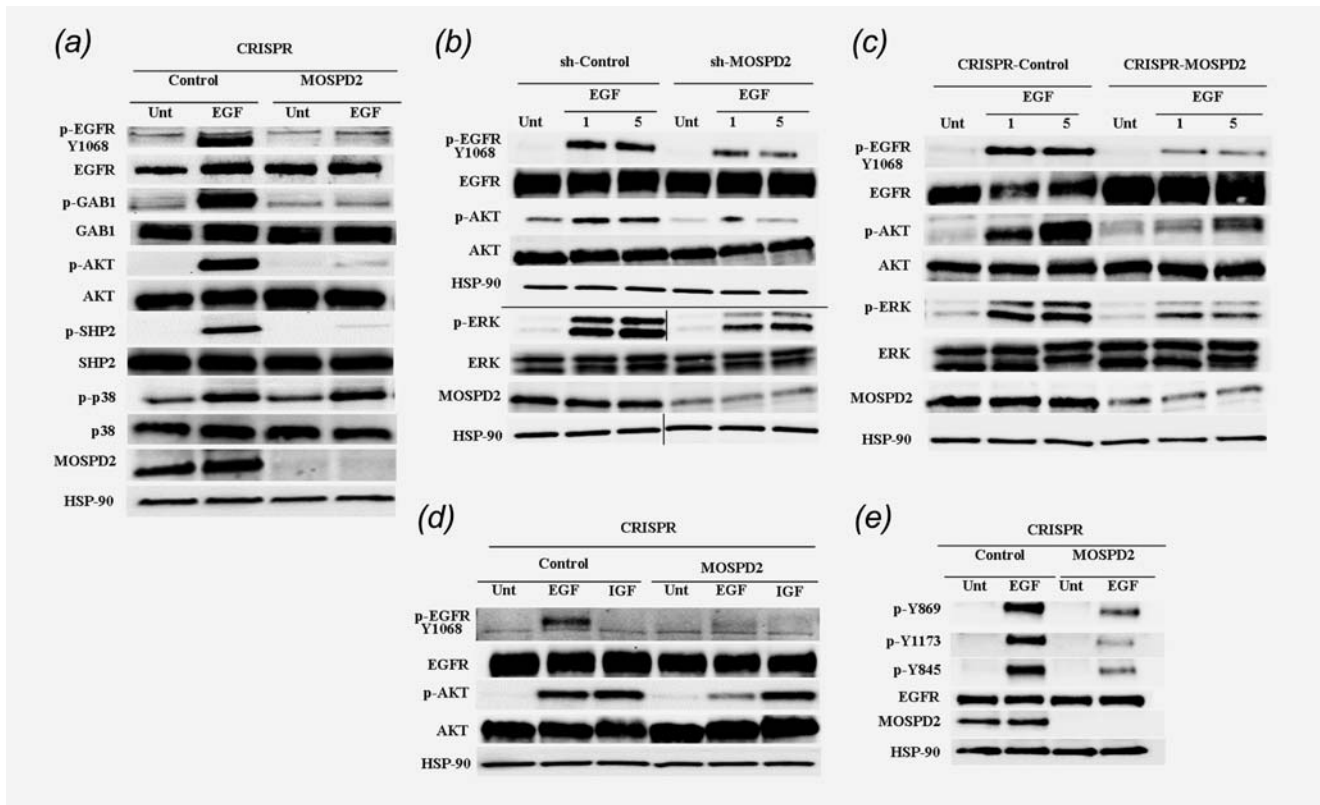


**Figure 4.** MOSPD2 is essential for EGF-induced signaling pathways in breast cancer cells. Western blots on MDA-231 breast cancer cells transduced with CRISPR-Control or CRISPR-MOSPD2 lentiviral particles and activated with EGF (*a*, *d* and *e*) or IGF (*d*) for 5 min. In *e*, the number of tyrosine residue on EGFR is indicated. One of 2–3 experiments is shown. BT-20 (*b*) and ZR-75-1 (*c*) control and MOSPD2-silenced cells were activated with EGF for 1 and 5 min. Phosphorylation of the EGFR and downstream cues are shown. EGF 20–200 ng/mL. One of three experiments is presented.

Several reports showed that blocking EGFR inhibits metastasis of breast cancer cells.<sup>9,20,21</sup> Other receptors, such as the chemokine receptor CXCR4, are also believed to be involved in breast cancer dissemination *in vivo*.<sup>22,23</sup> Yet, whereas pre-clinical studies targeting chemokine receptors or their ligands significantly inhibited breast cancer metastasis<sup>12,13</sup>, none of these treatments are currently implemented in the clinical setting. Moreover, strategies that were developed to target EGFR in cancers such as colon and head and neck, including the use of mAbs to block ligand binding, and small molecule tyrosine kinase inhibitors<sup>24–27</sup> were not approved for treatment of breast cancer. The failure to translate pre-clinical studies into clinical therapy aimed at averting the dissemination of tumor cells may stem, at least in part, from the promiscuity of receptors involved in their migration and the wealth of chemokines present in the cancer milieu. Identifying MOSPD2 as a protein that is ascribed to promoting migration induced by an array of chemokines (this manuscript and Ref. 14) may, therefore, lead to the development of strategies to block its expression and consequently circumscribe metastasis of tumor cells from different origins, including the breast. Moreover, the expression of such a protein on

the plasma membrane of tumor cells offers the potential application of immunotherapy strategies such as CAR-T cells and bi-specific antibodies to induce tumor destruction. The precise region in MOSPD2 that facilitates its function in breast cancer cells is currently unknown but it is of great importance to the further development of inhibitory compounds. Since MOSPD2 does not, presumably, incorporate a cytoplasmic tail, we speculate that it may pair with surface membrane proteins to serve as a co-receptor in a complex that is necessary to promote cancer cell chemotaxis migration. Different approaches are currently being taken to identify potential partners for MOSPD2.

Although most of our study focused on the triple negative cell line MDA-231, the data in this study indicate that MOSPD2 plays a role in the migration process of other breast cancer cells of different classifications. Furthermore, tumor microarray staining of MOSPD2 was, by in large, positive only in invasive and metastatic cells regardless of their classification. In view of these results, we propose using MOSPD2 as a potential target for the treatment of metastatic breast cancer by inhibiting migration and/or by eliminating MOSPD2<sup>+</sup> tumor cells.

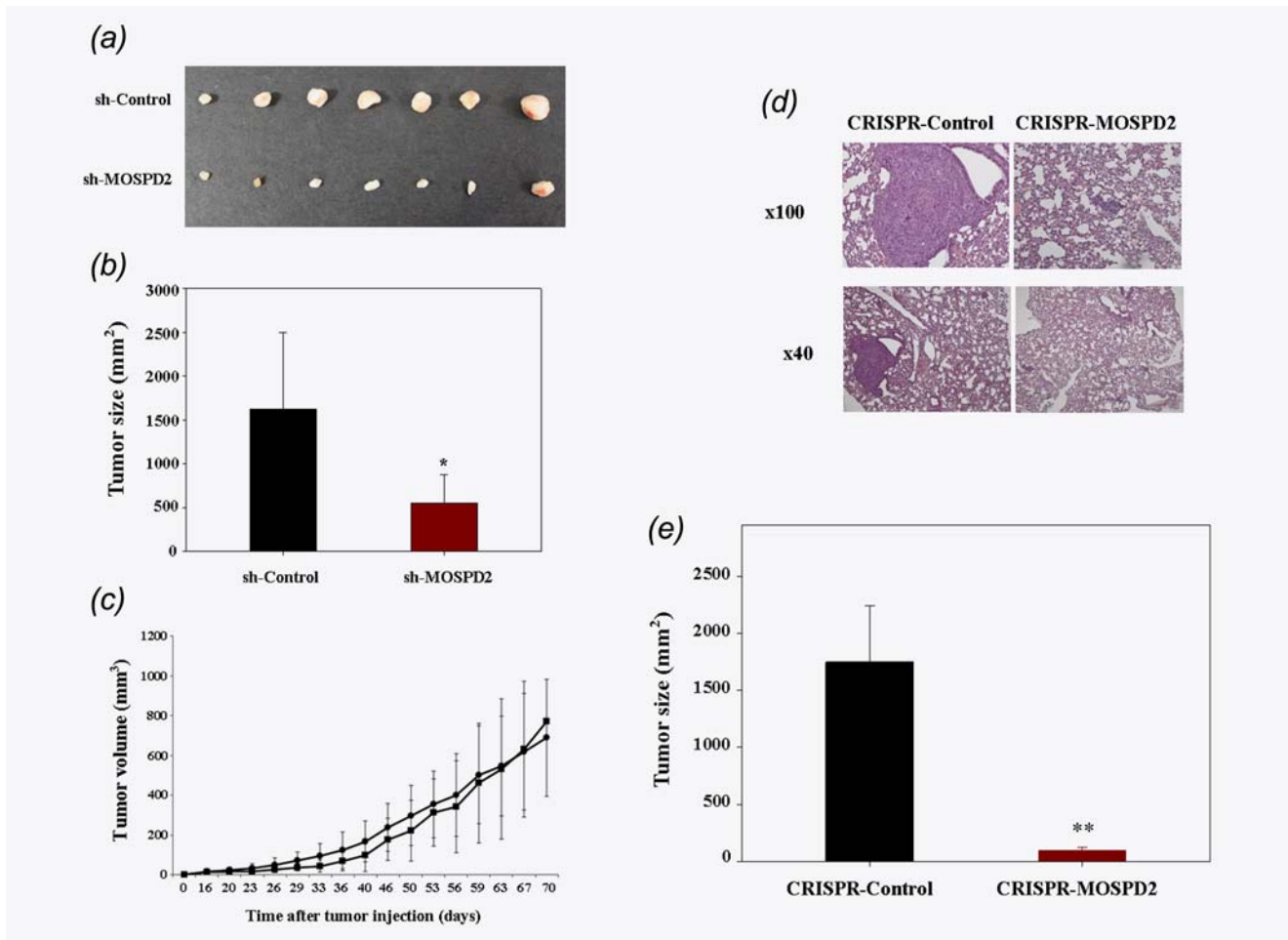


**Figure 5.** Mospd2 promotes metastasis of MDA-231 breast cancer cells. (a,b) SCID mice were injected in the mammary fat pad with MDA-231 breast cancer cells ( $5 \times 10^6$ ) transduced with sh-Control or sh-MOSPD2 lentiviral particles ( $n = 11$  and  $n = 8$ , respectively). Mice were sacrificed on day 70. The ipsilateral inguinal lymph node was excised (a), lungs were harvested for H&E staining, and the tumor area was determined (b). (c) Tumor volume comparison between mice orthotopically injected with CRISPR-Control or CRISPR-MOSPD2-treated MDA-231 cells. Tumor growth was monitored externally using caliper. Tumor volume = (length  $\times$  width<sup>2</sup>)/2. (d,e) SCID mice were injected into the tail vein with MDA-231 breast cancer cells ( $10^6$ ) transduced with Control-CRISPR or MOSPD2-CRISPR-isolated clone 14 ( $n = 11$  and  $n = 7$ , respectively). Mice were sacrificed after 3 weeks and their lungs were excised for histopathologic examination. The results shown are expressed as mean  $\pm$  standard error of measured metastasis size. Mean tumor area comprises the maximal lung tumor area measured for each mouse. \* $p \leq 0.05$ , \*\* $p \leq 0.005$ . [Color figure can be viewed at [wileyonlinelibrary.com](http://wileyonlinelibrary.com)]

## References

- Sporn MB. The war on cancer. *Lancet* 1996;347: 1377–81.
- Thiery JP. Epithelial-mesenchymal transitions in tumour progression. *Nat Rev Cancer* 2002;2: 442–54.
- Kalluri R, Weinberg RA. The basics of epithelial-mesenchymal transition. *J Clin Invest* 2009;119: 1420–8.
- Muller A, Homey B, Soto H, et al. Involvement of chemokine receptors in breast cancer metastasis. *Nature* 2001;410:50–6.
- Mukherjee D, Zhao J. The role of chemokine receptor CXCR4 in breast cancer metastasis. *Am J Cancer Res* 2013;3:46–57.
- Lyszkiewicz M, Witzlau K, Pommerenke J, et al. Chemokine receptor CX3CR1 promotes dendritic cell development under steady-state conditions. *Eur J Immunol* 2011;41:1256–65.
- Dewan MZ, Ahmed S, Iwasaki Y, et al. Stromal cell-derived factor-1 and CXCR4 receptor interaction in tumor growth and metastasis of breast cancer. *Biomed Pharmacother* 2006;60: 273–6.
- Chen HW, Du CW, Wei XL, et al. Cytoplasmic CXCR4 high-expression exhibits distinct poor clinicopathological characteristics and predicts poor prognosis in triple-negative breast cancer. *Curr Mol Med* 2013;13:410–6.
- Appert-Collin A, Hubert P, Cremel G, et al. Role of ErbB receptors in cancer cell migration and invasion. *Front Pharmacol* 2015; 6:283.
- Yarden Y, Pines G. The ERBB network: at last, cancer therapy meets systems biology. *Nat Rev Cancer* 2012;12:553–63.
- O'Hayre M, Salanga CL, Handel TM, et al. Chemokines and cancer: migration, intracellular signalling and intercellular communication in the microenvironment. *Biochem J* 2008;409: 635–49.
- Williams SA, Harata-Lee Y, Comerford I, et al. Multiple functions of CXCL12 in a syngeneic model of breast cancer. *Mol Cancer* 2010; 9:250.
- Tamura H, Hori A, Kanzaki N, et al. T140 analogs as CXCR4 antagonists identified as anti-metastatic agents in the treatment of breast cancer. *FEBS Lett* 2003;550:79–83.

14. Mendel I, Yacov N, Salem Y, et al. Identification of motile sperm domain-containing protein 2 as regulator of human monocyte migration. *J Immunol* 2017;198:2125–32.
15. Junttila MR, Mao W, Wang X, et al. Targeting LGR5+ cells with an antibody-drug conjugate for the treatment of colon cancer. *Sci Transl Med* 2015;7:314ra186.
16. Davidson NE, Gelmann EP, Lippman ME, et al. Epidermal growth factor receptor gene expression in estrogen receptor-positive and negative human breast cancer cell lines. *Mol Endocrinol* 1987;1:216–3.
17. Price JT, Tiganis T, Agarwal A, et al. Epidermal growth factor promotes MDA-MB-231 breast cancer cell migration through a phosphatidylinositol 3'-kinase and phospholipase C-dependent mechanism. *Cancer Res* 1999;59:5475–8.
18. Karamouzis MV, Papavassiliou AG. Targeting insulin-like growth factor in breast cancer therapeutics. *Crit Rev Oncol/Hematol* 2012;84:8–17.
19. Dunn SE, Ehrlich M, Sharp NJ, et al. A dominant negative mutant of the insulin-like growth factor-I receptor inhibits the adhesion, invasion, and metastasis of breast cancer. *Cancer Res* 1998;58:3353–61.
20. Salcedo R, Martins-Green M, Gertz B, et al. Combined administration of antibodies to human interleukin 8 and epidermal growth factor receptor results in increased antimetastatic effects on human breast carcinoma xenografts. *Clin Cancer Res* 2002;8:2655–65.
21. Antonyak MA, Li B, Regan AD, et al. Tissue transglutaminase is an essential participant in the epidermal growth factor-stimulated signaling pathway leading to cancer cell migration and invasion. *J Biol Chem* 2009;284:17914–25.
22. Liang Z, Wu T, Lou H, et al. Inhibition of breast cancer metastasis by selective synthetic polypeptide against CXCR4. *Cancer Res* 2004;64:4302–8.
23. Li YM, Pan Y, Wei Y, et al. Upregulation of CXCR4 is essential for HER2-mediated tumor metastasis. *Cancer Cell* 2004;6:459–69.
24. Van Cutsem E, Peeters M, Siena S, et al. Open-label phase III trial of panitumumab plus best supportive care compared with best supportive care alone in patients with chemotherapy-refractory metastatic colorectal cancer. *J Clin Oncol* 2007;25:1658–64.
25. Moore MJ, Goldstein D, Hamm J, et al. Erlotinib plus gemcitabine compared with gemcitabine alone in patients with advanced pancreatic cancer: a phase III trial of the National Cancer Institute of Canada Clinical Trials Group. *J Clin Oncol* 2007;25:1960–6.
26. Sequist LV, Yang JC, Yamamoto N, et al. Phase III study of afatinib or cisplatin plus pemetrexed in patients with metastatic lung adenocarcinoma with EGFR mutations. *J Clin Oncol* 2013;31:3327–4.
27. Van Cutsem E, Kohne CH, Hitre E, et al. Cetuximab and chemotherapy as initial treatment for metastatic colorectal cancer. *N Engl J Med* 2009;360:1408–7.